AIFA - UNIVERSITÄT BONN

Supervisor :

Prof. Dr. Norbert Langer

Transport of angular momentum in massive stars during their main sequence evolution

Bachelor of Science Thesis by

Marius Mürz

August 2013

Abstract

In this thesis I analyse the change of the angular momentum at the surface of massive, main sequence stars on the basis of the observational data from the VLTS-FLAMES-Survey, during this thesis "massive" means between 12 - 20 $M_{\odot}$(**?**).

The idea is to divide main sequence stars of 12-20 $M_{\odot}$ into 2 groups of roughly equal number with respect to their progress on their main sequence evolution. Then for the first, in their main sequence evolution less progressed, group the surface rotation velocity can be predicted for a later stage. This prediction is based on assumptions about the transport of angular momentum in stars during their main sequence. In this thesis two assumptions have been tested, the first one is that stars have no angular momentum transport at all, and the second one treats stars as rigid rotators. The rotational velocity distribution of the first group can be compared to the observational velocity distribution of the second group of massive main sequence stars.

Depending on the accordance of the theory with the observations, conclusions will narrow down the possibilities of how the angular momentum transport in stars could occur. Both predicted distributions differ from the observational data of the second group. The calculated distribution of the rotational surface velocity for no angular momentum transport has too many slow rotators and the rigid rotator distribution has to many fast rotators to fit the data. This implies that stars must have some angular momentum transport, since the first assumption does not fit the data, but it is not instantaneous since the stars are not rigid rotators.

Correctors

1 Corrector : Prof. Dr. Norbert Langer - AIfA - Universität Bonn

2 Corrector : Dr. Ilka Petermann - AIfA - Universität Bonn

Contents

Chapter 1

Introduction

1.1 Motivation

Humanity was always curious about a great many things we found in nature. There are three kinds of questions that always are asked, when something new is discovered :

- What is its effect?
- How is it working?
- What is its origin?

The scientific answer to the last question for most things humanity discovered is : The remains of a star.

The elements formed after the Big Bang were hydrogen, helium and a small amount of lithium, with the abundances $H = 0.762$, $He = 0.238$ and $Li = 1.3 \cdot 10^{-10}$ (Langer, 2012a). From these elements the first generation of stars formed. After burning their hydrogen content in the core, hydrogen burning ceases. The helium core burning starts, and the first heavy elements were created. Most of these stars were very massive, above 60 $M_{\odot}$(de Mink, 2010), and therefore end their life violently in a supernova explosion. The fused elements where blown into the universe and enriched it with metals, in astronomical terms metal includes all elements heavier than helium.

Many heavy elements are produced in stars. The heaviest element produced through nuclear fusion is iron. All heavier elements are either produced in supernova explosions or through neutron-capture(Pols, 2009). Therefore the earth and all living things consist of the remains of long gone stars. The carbon in our cells, as well as the oxygen we breathe, are ashes of burning processes in stars. So stars are indeed a very interesting and important part of the universe.

1.2 The observation of stars

There is only one way to achieve knowledge in science: observation. Without the consent with observations theories are only words without substance.

Since the beginning mankind looked at the stars, but only a century ago the first quantitative classification of stars were done by Hertzsprung (1911) and Russell (1913)(de Mink, 2010). The listed observed stars with their absolute brightness and color, and created the Hertzsprung-Russell diagram that has been used by astronomers ever since. The Hertzsprung-Russell diagram is mostly used to understand the evolution of stars.
Today we know the distance to many star clusters. If the distance to a star is known, the absolute brightness can be used to calculate the luminosity of a star. The color of a star can be converted into a spectral type, or furthermore into an effective surface temperature. Now the stars of different distances can be compared in one Hertzsprung-Russell diagram. For the lower mass stars, those which do not end in supernova, the evolution is well predicted by models. For the massive stars, this is not the case. The distribution of massive stars predicted by the models seems to differ significantly from the observed stars(de Mink, 2010).

1.3 Aim of this thesis

Rotation has a huge impact on the evolution of a massive star. Through the centrifugal force, the effective mass is reduced, this leads to a decrease in the luminosity (Langer, 2012b) of a star. The rotation can induce mixing, leading to a rejuvenation and hence, a longer lifetime of the star(Pols, 2009). The influence of rotation on a massive star is as strong as the influence of the mass and the metallicity(Langer, 2012b). Therefore it is important to understand the rotation of massive stars, in order to understand the evolution of the stars themselves. Since hydrogen burning lasts for 90% of the lifetime of a star, the main sequence phase, roughly 90% of the observed stars should be on their main sequence. Hence the main sequence evolution of the stars is the most interesting part. This thesis will test two ways of angular momentum transport in massive stars during their main sequence in their prediction of the rotational surface velocity. This will be done by predicting a distributions of rotation velocities for roughly 40 stars, and comparing it to observations from the VLTS-FLAMES survey.

Chapter 2

Properties of rotating massive stars

2.1 Star formation - initial angular momentum

A star is born when a part of an interstellar gas cloud reaches the Jeans limit(Pols, 2009). At this point the proto star's gravitation exceeds the ideal gas pressure and the cloud collapses to the point the central temperature reaches roughly 10^7 Kelvin.(Pols, 2009) Now hydrogen burning starts and thus the main sequence evolution of the star. Through his whole evolution the star remains in hydrostatic equilibrium (Pols, 2009).
The angular momentum in the star, is related to the gas particles in the interstellar cloud from which the star has been formed. Therefore stars can have a different initial angular momentum and a different initial rotational velocity on their surface.

2.2 Transport of angular momentum

2.2.1 Mixing by differential rotation

When a massive star begins its main sequence evolution, in the center hydrogen is fused to helium through the CNO-cycle. During the main sequence evolution the envelope of the star expands, but the core contracts. If there would be no angular momentum transfer in the star the surface velocity would decrease by the expansion factor c but the rotation velocity of the core would increase, because the core is shrinking. This would lead to differential rotation. The result would be local mixing between to mass shells(Pols, 2009).

2.2.2 Convective mixing

Hydrogen burning needs a temperature of roughly 10^7 K. In a sphere of gas, that is held together by its own gravity, and is in both hydrostatic and thermal equilibrium, the temperature is highest where the density is highest, in the core. This holds only for non degenerate stars. Therefore nuclear burning only occurs in the center, most of the produced energy is stored in thermal energy and needs to find its way through the star to the surface. One way of heat transport in a star is photon diffusion. If the temperature gradient in the star exceeds the radiative gradient, which is given by the limited energy transport through photons, convection sets in as a cooling mechanism. Convection is a process where huge

blobs of gas form and do the same thing as a balloon in our atmosphere. They rise, in response the same volume of gas sinks down into the interior of the star. These blobs have a high temperature and rise in regions with lower temperatures until the disperse, and after they assimilate their temperature with the local surroundings. This process moves mass and thermal energy efficiently through convective layers of a star, those layers where the temperature gradient is steep(Pols, 2009).

Mixing implies mass motion, and with the mass travels the angular momentum. Without mixing and mass transfer the angular momentum in the core of rapidly rotating stars would reach critical rotation (Langer, 2012b) and v_{rot} would decrease at the surface of the expanding envelope. If the angular momentum would reach the surface, due to mixing, the surface would receive more angular momentum and would lose less speed during the expansion of the envelope.

2.3 Stellar winds - loss of angular momentum

Stars with higher mass than 25 $M_\odot$ have significant mass loss during their main sequence evolution and end as Wolf-Rayet stars (Pols, 2009).

2.3.1 Precondition for mass loss

The star stays in hydrostatic equilibrium during its evolution, the only thing that holds it together is its own gravity. A non-zero rotational velocity at the surface reduces the effective gravity at the equator through the centrifugal force. As the envelope expands during the star's evolution, the gravitational force at the stellar equator becomes weaker.

2.3.2 Wind driving mechanisms

If the mass is weakly bound, strong photon flux can eject mass from the star, this process is called line driving(Pols, 2009).
The line driving mechanism works best if the star is metal rich, and therefore when the surface has a high metallicity. A star is metal rich, if the gas cloud it was born in, was enriched by the burning ashes of massive stars, that died in a supernova explosion. As the heaviest element produced through fusion in stars, iron is the strongest line driving element. Due to its many absorption lines iron has a larger spectral width of photons that can be absorbed than the lighter elements found in stars. The driving mechanism itself works due to momentum conservation, the translative momentum of the photons that are absorbed by the atoms in the envelope carry a momentum which will be transferred to the atoms. The more photons the atoms absorb, the more momentum they get, and the larger the acceleration out of the star. Due to a non zero velocity of the absorbing atoms in the envelope the absorption lines get broadened by the Doppler effect. This increases the efficiency of the line driving mechanism, because even more photons can be absorbed.

Once the mass is ejected, the star has a new surface layer that may rotate faster or slower then the old one, since the only mensurable rotational velocity is the rotational surface velocity, this is important.

2.3.3 Magnetic breaking

Convection, differential rotation and many not fully understood processes in stars can give rise to magnetic fields(Langer, 2012b). In general magnetic fields are produced by moving charged particles, or currents. Convection produces local magnetic fields, if the surface layers of star is convective, this will lead to magnetic fields at the surface(Langer, 2012b).

If there is a stellar wind of charged particles leaving the star, and a strong magnetic field, the star will slow itself down. The charged wind will interact with the magnetic field as it is driven away from the star. The magnetic field and the star are bound in rotation, they have the same angular velocity. The angular velocity of the wind in respect to the rotation axis of the star will stay the same as on the envelope. It will then move in respect to the magnetic field and induce a torque on the star, due to its inertia. If the wind is strong and the magnetic fields are strong, it slows down the star significantly(N. Langer, private communication).

2.4 Binary effects

According to Langer (2012b) the fraction of close binaries between the massive stars is very large, between 45% and 75 % for O type stars. With 90% of these binaries being close enough for one star to fill its Roche-lobe during their life, binary interaction is very important in massive star evolution.

When mass transfer occurs, an accretion disc will form around the mass gainer (Langer, 2012b) and with the mass angular momentum will be transported from the mass donor to the mass gainer. This can lead to critical rotation of the mass gainer and therefore stop the mass accretion.

The second big impact on the rotation of a massive star in a binary is the merging of these stars. About 25% of the O type binaries will produce a merger(Langer, 2012b). Many of these mergers are rapid rotators and because it is difficult to separate them from observed massive single stars, they contribute to the problems with understanding massive single star evolution.

Chapter 3

Methods

3.1 Observational data

The data used for this thesis comes from the VLT-FLAMES Survey. In the survey originally over 500 massive stars in the LMC, SMC and MW where observed(Evans et al., 2005). The survey was started to obtain rotation rates, radial radiation variation for binaries and surface abundances for a large sample of O and B stars to progress the understanding of massive star evolution. The tool of observation was the VLT and most measurements where spectral analysis of the stars. Here I consider only the data for stars of the relevant mass range, 12 - 20 $M_{\odot}$. This thesis focuses on the massive stars, therefore stars below 12 $M_{\odot}$ were not used. A massive star is a star that avoids the fate of a white dwarf, and instead ends its life in a core collapse supernova. The lower mass limit for massive stars is roughly 8 $M_{\odot}$. Since the mass was obtained observationally, the exact mass is uncertain. Therefore the lower limit was lifted from 8 to 12 $M_{\odot}$ to make sure no low mass stars are in the sample. Above 25 $M_{\odot}$ the mass loss during the main sequence evolution increases (Pols, 2009) and has a big effect on the change of the rotational surface velocity of the stars, hence these stars also were not used. The reason to stop at 20 $M_{\odot}$ is the low number of stars above this mass, making statistical analysis difficult. Also stars that clearly left the main sequence where not used. This was determined by retrieving the radius of a star at the end of its main sequence evolution from the model files of Brott et al. (2011). These model files where calculated for comparison with the VLTS FLAMES survey. The metallicity equals the composition of the LMC and the calculation include the effects of rotation in massive star evolution.

To enhance any effects occurring during the main sequence evolution of the stars, the stars in the middle of their main sequence evolution also were not used. The definition of this middle differs for each mass and will be defined in the next paragraph. The first group of stars is defined as stars at the start of their main sequence evolution, and the second group as stars near the end of their main sequence evolution. The sample for this thesis includes 91 stars with measurements of the effective temperature, luminosity, surface rotation velocity and total mass.
These relevant stars have been divided into two groups based on the fraction of their lifetime on the main sequence that already passed. A threshold time $t_{thr,i}(M)$ has been defined :

$$t_{thr,i}(M) = t_{MS}(M) \cdot \frac{a_i}{100} \tag{3.1}$$

Where $t_{MS}(M)$ is the time a star of the mass M spends on the main sequence taken, from models (Brott et al., 2011) for masses 12 ,13 ,15 ,16 ,19 and 20 $M_{\odot}$. The parameter a_i is a constant and was chosen to balance the total number of stars in both groups for better statistical comparison and keep it at roughly 45 stars per group. The a_i are divided by 100 to write them as percentage of the main sequence time. To divide the sample two threshold times are needed. One to define the upper limit of the first group, $t_{thr,1}$. And the other one to define the lower limit of the second group, $t_{thr,2}$. The upper limit of the second group is simply t_{MS} and the lower limit of the first group is $t = 0$.
Since two threshold times are needed, one also needs two parameters a_i with $a_1 = 64$ and $a_2 = 87$. These have been estimated through trial and error. This means the stars in the first group are at an earlier state of evolution than the stars in the second group.
$t_{MS}(M)$ could not be obtained for all masses because the corresponding tracks were not accessible. To obtain the correct time anyway, the known times have been plotted against the mass and a simple power law ($t_{MS}(M) = a \cdot M^2 + b \cdot M + n$) seems to fit the data quite well (Figure 3.1 and Table 3.1).
The age threshold can be translated into a radius threshold. This is helpful, because the age of the observed stars is not known, but the radius can be calculated from the effective temperature and luminosity. $R_{thr,i}(M)$ can be obtained from the corresponding model and represents the radius of the model with mass M and age $t_{thr,i}(M)$. The threshold radii for both threshold times are displayed in Table 3.1.

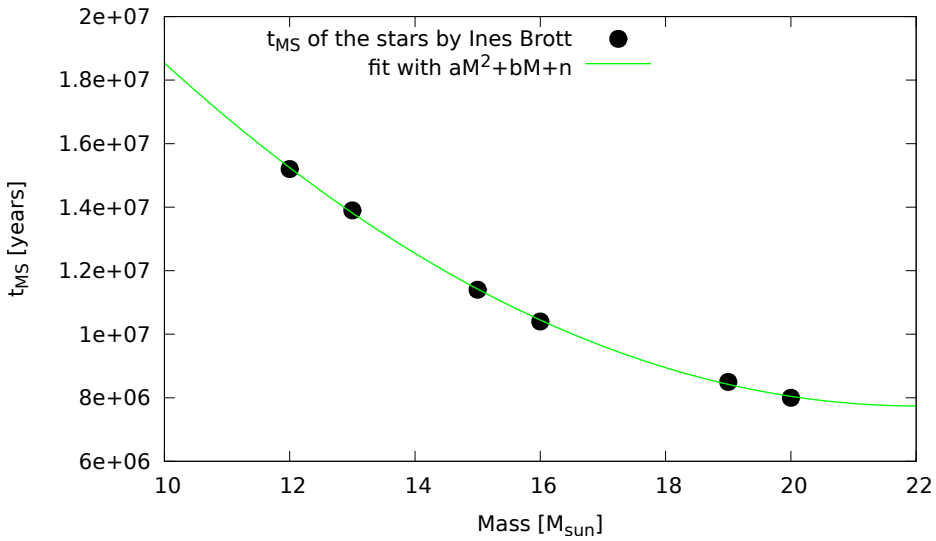

Figure 3.1: The main sequence lifetime for a star as function of its initial mass in Solar masses shows a non linear dependence. The green line illustrates the polynominal law, the dots represent the lifetimes obtained from the models. The parameters solved for a = 74700 ± 5100 years, b = -32.9 ± 1.6 $\cdot 10^5$ years and n = 44 ± 1.3 $\cdot 10^6$ years.

Table 3.1: The resulting lifetime of the main sequence (t_{MS}, second column) and the resulting threshold times ($t_{thr,i}$, third and forth column) in years and the threshold radius (R_{thr}, forth and fifth column) in $R_{\odot}$ for all masses (M) in solar mass (first column). The red values of t_{MS} are the calculated ones. The threshold times have been calculated by equation 3.1.

M [$M_\odot$]	t_{MS}(M) [y]	$t_{thr,1}$(M) [y]	$t_{thr,2}$(M) [y]	$R_{thr,1}$(M) [$R_\odot$]	$R_{thr,2}$(M) [$R_\odot$]
12	$1.52 \cdot 10^7$	$9.72 \cdot 10^6$	$1.32 \cdot 10^7$	5.27	7.53
13	$1.39 \cdot 10^7$	$8.89 \cdot 10^6$	$1.21 \cdot 10^7$	5.99	8.7
14	$1.25 \cdot 10^7$	$8.03 \cdot 10^6$	$1.09 \cdot 10^7$	6.29	9.2
15	$1.14 \cdot 10^7$	$7.33 \cdot 10^6$	$9.96 \cdot 10^6$	6.6	9.7
16	$1.04 \cdot 10^7$	$6.66 \cdot 10^6$	$9.05 \cdot 10^6$	6.93	10.25
17	$9.62 \cdot 10^6$	$6.16 \cdot 10^6$	$8.37 \cdot 10^6$	7.16	10.65
18	$8.95 \cdot 10^6$	$5.73 \cdot 10^6$	$7.78 \cdot 10^6$	7.39	11.05
19	$8.50 \cdot 10^6$	$5.44 \cdot 10^6$	$7.39 \cdot 10^6$	7.62	11.46
20	$8.00 \cdot 10^6$	$5.12 \cdot 10^6$	$6.96 \cdot 10^6$	7.82	11.89

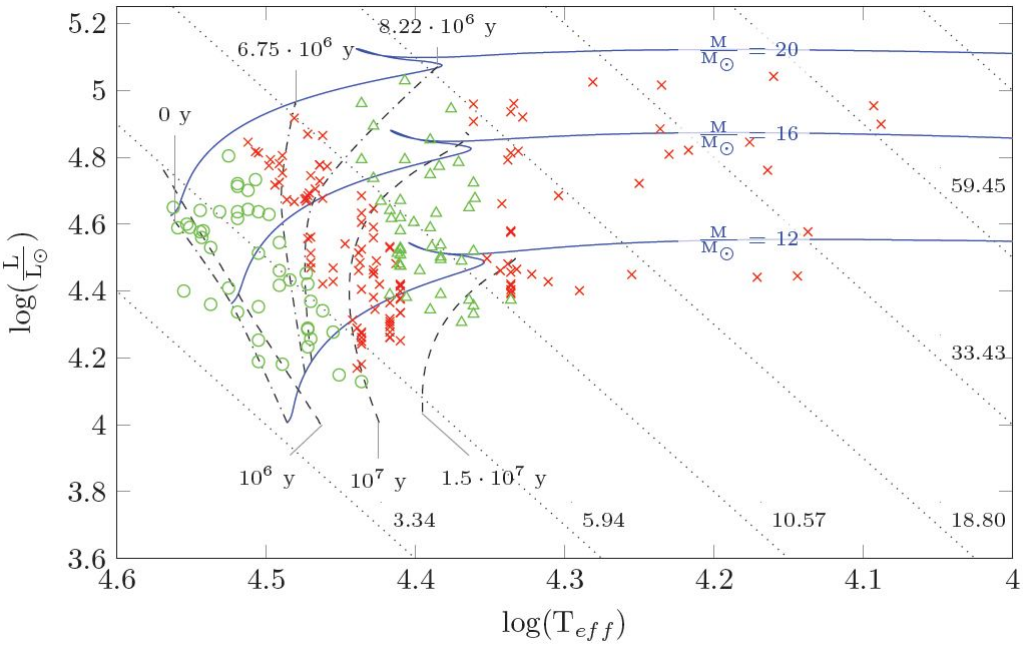

Figure 3.2: Solar luminosity of the red stars with mass between 12 - 20 $M_\odot$ and their logarithmic effective temperature are used to display the stars. Lines of constant radii (dotted) labelled with values of $\frac{R}{R_\odot}$ and evolutionary blue models for 3 different masses with overshooting are shown. Isochrones calculated by Brott et al. (2011)(dashed lines) and isochrons extrapolated only from the 3 models (dashdotted) indicate the age of the stars. The green ∘ represent stars of the early group, the green △ stars of the late group.

The stars can now be separated into two groups : The early group and the late group. In a Hertzsprung-Russell diagram (HRD) one can verify the evolutionary state of the stars in both groups (Figure 3.2).
For both groups the rotational velocities are displayed in a histogram (Figure 3.3).
There are more fast rotators in the early group than in the late group, and the other way around with the slow rotators.
The aim was to approximate the angular momentum transport in these stars during their main sequence evolution by a simple assumption. To find a criterion of the main sequence evolution progress for the two groups, one needs the average radii of the stars in the two groups.

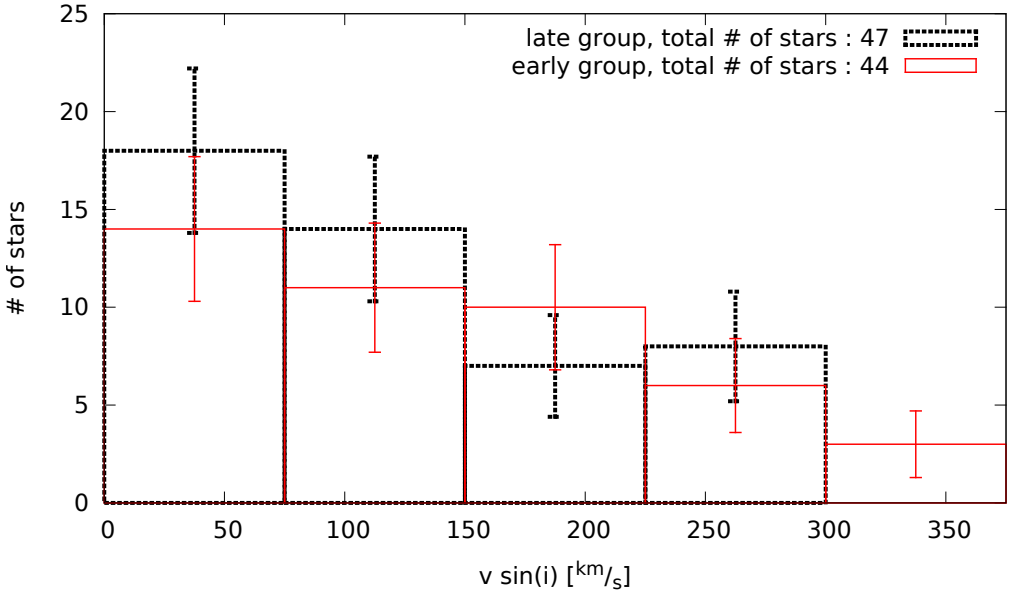

Figure 3.3: These histograms show the observed rotational velocity distributions for the early and the late group (dotted) of the stars. The bin width is 75 km s^{-1} and the errorbars are poisson errors with $\Delta N = \sqrt{N}$.

3.2 Determining the average radius

To compare the rotational velocity distributions of two groups of stars one needs to find an average factor that describes the velocity change from the early group to the late group. Because the velocity change is highly depending on the change of the radius of the star, it is necessary to find an average radius for each group and each mass. This radius change itself depends on the mass of the star, hence the stars have been divided into mass bins and the average radii have been calculated for each bin separately as

$$\begin{aligned} \overline{R}_E(M) &= \frac{\sum_{i=1}^{N_E(M)} R_{E,i}(M)}{N_E(M)}, \\ \overline{R}_L(M) &= \frac{\sum_{i=1}^{N_L(M)} R_{L,i}(M)}{N_L(M)}, \\ c(M) &= \frac{\overline{R}_L(M)}{\overline{R}_E(M)}, \end{aligned} \tag{3.2}$$

with $N_E(M)$ being the total Number of stars with $R_i(M) < R_{thr,1}(M)$ and $N_L(M)$ for $R_i(M) > R_{thr,2}(M)$ for the current stellar mass M. $c(M)$ is the average expansion factor between the early and the late group. Unfortunately for some masses (18 and 20 $M_\odot$) there was no data in the late group. Therefore the average radius could not be calculated. The $c(M)$ factor in this case was approximated, this is possible, because the factor does not change much with the stellar mass.

Table 3.2: c(M) was calculated by Equation 3.2 and is the expansion factor for each mass. The average radii for early and late group and the given mass M are given in $R_\odot$. $N(M)$ is the number of stars in each mass bin M.

M [$M_\odot$]	$\overline{R}_E(M)$ [$R_\odot$]	$N(M)$	$\overline{R}_L(M)$ [$R_\odot$]	$N(M)$	c(M)
6	5.09 ± 0.36	2	8.98 ± 0.27	11	1.77 ± 0.19
13	5.37 ± 0.22	6	9.77 ± 0.35	8	1.82 ± 0.14
14	5.45 ± 0.31	3	10.36 ± 0.35	9	1.90 ± 0.18
15	5.21 ± 0.18	8	11.84 ± 0.42	8	2.27 ± 0.16
16	5.73 ± 0.33	3	13.03 ± 0.75	3	2.28 ± 0.26
17	6.16 ± 0.31	4	12.40 ± 0.62	4	2.01 ± 0.20
18	5.67 ± 0.20	8	17.55 ± 1.75	1	3.09 ± 0.46
19	6.02 ± 0.21	8	13.01 ± 1.30	1	2.16 ± 0.32
20	6.41 ± 0.45	2	15.16 ± 1.07	2	2.37 ± 0.33

Since the stars are divided into two groups with known average radii and expansion factors for each mass, one can start with the two extreme assumptions :

1 The angular momentum of each mass shell is assumed to be constant (no angular momentum transport)

2 The star is assumed to be a rigid rotator (instantaneous transport of angular momentum throughout the star)

3.3 No angular momentum transport

The key to the prediction of the rotational velocity of the star v_{rot} is the average stellar radius $\overline{R}_E(M)$ in the early and the late group $\overline{R}_L(M)$, the mass M and the constant angular momentum in a mass shell L. If this mass shell is the surface shell, then the constant angular momentum in the shell and the moment of inertia I can be used to find the a prediction for the rotational surface velocity after a change in the radius.

$$\begin{aligned} L = constant &= I\frac{v_{rot}}{R} \\ \Leftrightarrow v_{rot} &= \frac{LR}{I} \\ \text{with } I &= \frac{2}{3}R^2\mathrm{d}m \text{ for a thin shells} \\ \Rightarrow \frac{v_{rot,E}}{v_{rot,L}} &= \frac{\overline{R}_L(M)}{\overline{R}_E(M)} = c. \end{aligned} \quad , \tag{3.3}$$

Now one can easily evolve the rotational surface velocity distribution of the early group by dividing each rotation velocity by the factor c seen in Equation 3.2, and compare the result with the rotational surface distribution of the late group.

3.4 Rigid rotation

The assumption of a rigidly rotating star is the other extreme assumption. In this case the angular momentum is assumed to be transported instantaneously through the star. The

prediction of the velocity chance for an evolving star involves the calculation of its density profile for the time its radius reaches $\overline{R}_E(M)$ and $\overline{R}_L(M)$. The models of Brott et al. (2011) will be used.
One can then compute the moment of inertia of the stars and once again calculate a factor of rotational velocity change with a given change in the radius and the density profile $\rho(r)$. With the surface velocity v_{rot}, R the radius of the star, the angular momentum of the whole star L, the angular velocity of the star ω, a constant for a rigid rotator, and its moment of inertia I the change of the rotational velocity on the surface at the late stage $v_{rot,L}$ can be calculated from the velocity at the early stage $v_{rot,E}$. The first step is to equate L and to fill in ω and the moment of inertia I, this time in integral form and for the whole star. To the integral over the mass is converted into an integral over the volume V of the star, transformed into spherical coordinates.

$$
\begin{aligned}
L = \omega I &= \frac{v_{rot}}{R} \int_0^M r^2 \,\mathrm{d}m = \frac{v_{rot}}{R} \int_0^V \rho(r) r^2 \,\mathrm{d}V \\
\Rightarrow v_{rot} &= \frac{LR}{\int_0^V \rho(r) r^2 \,\mathrm{d}V} = \frac{LR}{4\pi \int_0^R \rho(r) r^4 \,\mathrm{d}r} \\
\Rightarrow v_{rot,L} &= v_{rot,E} \cdot \frac{\overline{R}_L(M)}{\overline{R}_E(M)} \cdot \frac{\int_0^{\overline{R}_E(M)} \rho_E(r) r^4 \,\mathrm{d}r}{\int_0^{\overline{R}_L(M)} \rho_L(r) r^4 \,\mathrm{d}r} = v_{rot,E} \cdot c(M) \cdot inte(M)
\end{aligned}
\tag{3.4}
$$

The *inte* factor can be calculated numerically from model profiles by slicing the star in thin mass shells (ca. 1300), using a simple trapezium method and assuming $\rho = constant$ for each shell. The expansion factor $c(M)$, is again calculated by Equation 3.2.
The problem is that once again *inte*(M) depends on the stellar mass, as c(M). c(M) has been dealt with in 3.2, now the *inte*(M) factors for each mass are needed. Profiles have been used to calculate the integral form of the moment of inertia of the density. And the profiles for masses 12, 13, 15, 16, 19 and 20 $M_\odot$where available, those for masses 14, 17 and 18 $M_\odot$ not. The achievable *inte*(M) factors can be found in Figure 3.4.

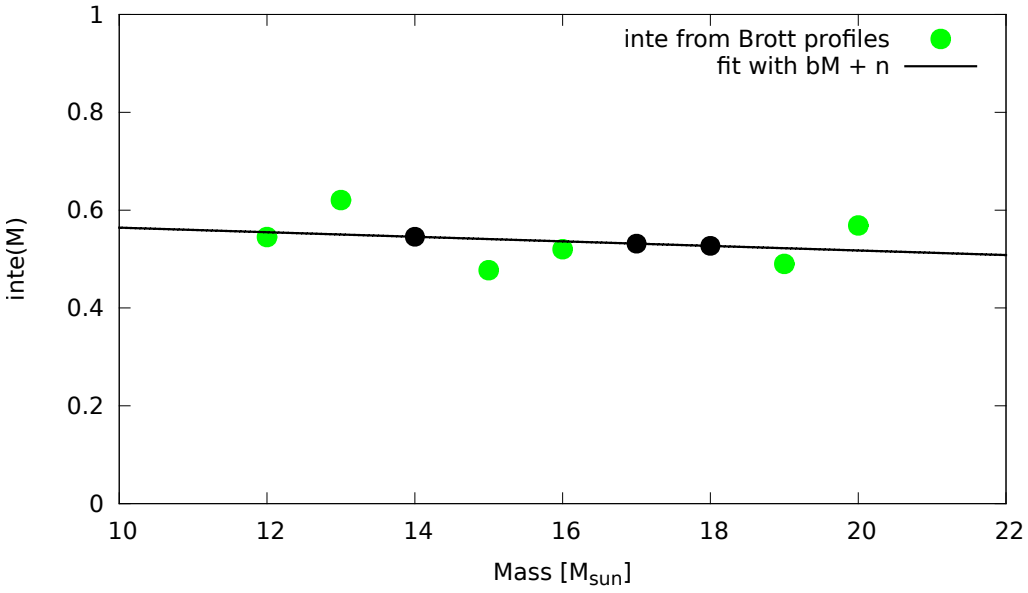

Figure 3.4: The *inte* factors mass dependence seems to be linear and has been approximate with a function $inte(M) = b \cdot M + n$. The green dots represent the *inte* factors calculated from the profiles by Equation 3.4 and the black dots are approximated by the linear law displayed in black.
The parameters solved for : b = -0.010 ± 0.0094, n = 0.54 ± 0.15

A linear approximation for the mass dependence of the *inte* factor has been made.

The missing *inte* factors have been calculated using the approximation.

Table 3.3: The first column shows the stellar mass, the second column the $inte(M)$ factors calculated in respect to that mass by equation 3.4. The numbers in red are the approximated *inte* factors.

M [$M_\odot$]	$inte(M)$
12	0.545 ± 0.042
13	0.621 ± 0.034
14	0.545 ± 0.171
15	0.477 ± 0.024
16	0.520 ± 0.042
17	0.531 ± 0.187
18	0.526 ± 0.193
19	0.490 ± 0.052
20	0.569 ± 0.057

3.5 An outlook

These two assumptions are extreme cases and are not expected to describe stars very well. no angular momentum transport would imply no mixing in stars. A rigid rotator would imply instantaneous mixing throughout the whole star. There is no evidence for neither of this two extreme cases. To really understand the transport of angular momentum it is necessary to use many more assumptions. A first step would be a superposition of the two extreme assumptions and then a numerical fit of the result to the observed data. Construction a new factor predicting the rotational velocity change

$$b(M) = \alpha(M) \cdot \frac{1}{c(M)} + \beta \cdot inte(M) \cdot c(M)$$

Then the weights α and β would tell how much stars would behave like a rigid rotator, and how much as they had no angular momentum transport.

Chapter 4

Results

4.1 Calculation of the theoretical velocity distributions

The observational data has been (as described in Section 3.1) divided into the early and the late group and the velocity distributions have been arrayed for both groups. The next step is to chose an assumption, either rigid rotation or no angular momentum transport. In Section 3.3 and Section 3.4 has been shown how to predict the rotational velocity change corresponding to the change of radius and density profile from the early to the late group. With use of the average radii of the groups, calculated in Section 3.2 the calculation is now only a matter of multiplying each velocity in the observed distribution with the corresponding factors. It is legitimate to simply multiply each velocity, because the factors have been calculated only with average values in respect to the mass of a star.
Due to the limited resolution of a histogram the comparison of the calculated rotation velocity distribution and the observed rotation velocity distribution of the late group will be done with cumulative distributions, rather than with histograms.
To get this cumulative distributions from the data one simply has to choose a group of stars and list their rotation velocities sorted descending. This one column of velocities can be converted into a cumulative distribution with the help of a small code that increases one parameter (v_i) from 0 to v_{max}, where v_{max} is the biggest rotational velocity in the group of stars, and then counts how many stars have a lower rotational velocity as the increasing v_i, this count is then plotted against the v_i.

For the cumulative distributions of the data one just skips the multiplying of the velocity change factors, and immediately sorts and converts the histogram.

4.2 Comparing to the observational data

After achieving the cumulative distributions for the data and the theory, they can be compared.

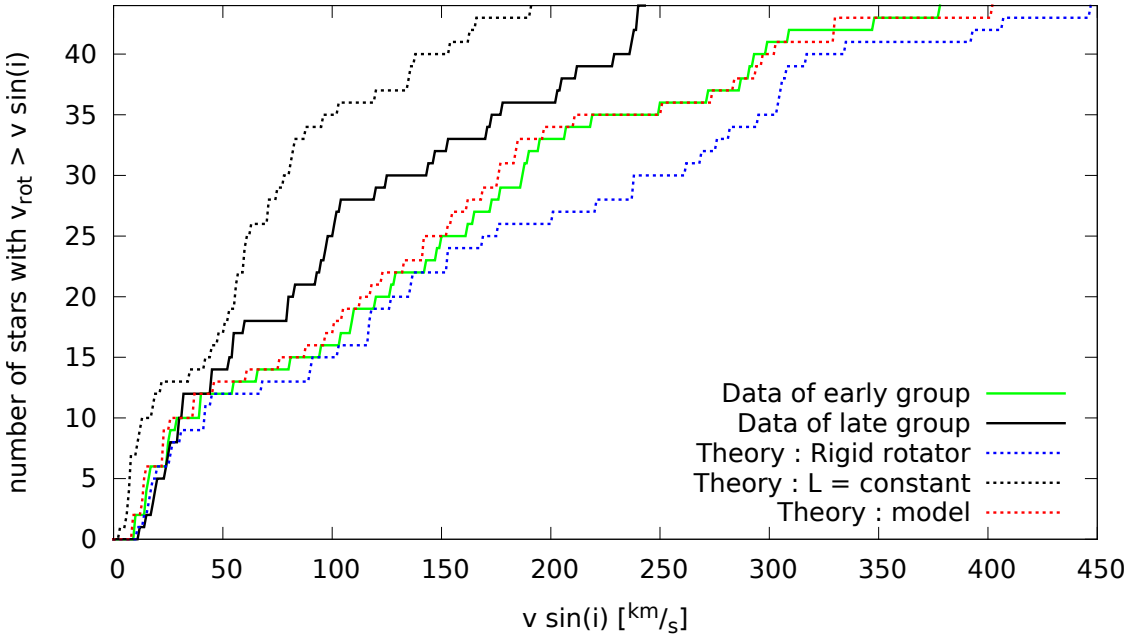

Figure 4.1: On the vertical axis is the number of stars with a bigger rotational surface velocity than then the velocity on the horizontal axis. The green solid line displays the observed rotational velocity distribution of the early group, the black solid line the observed distribution of the late group. The dotted lines represent the calculated distributions where the blue dotted line is calculated with the assumptions of a rigid rotator, and the the black dotted line with the assumption of no angular momentum transport. The theoretical distributions have been calculated with the expansion factors $c(M)$ in Table 3.2 and the $inte(M)$ factors in Table 3.3. The red dotted line represents a rotational velocity change described by models of Brott et al. (2011).

The goal was to approximate the change of the rotation velocity, and hence the change of the angular momentum in the surface of a star, by two assumptions and compare it to the data to see what fits best.

4.2.1 L = constant - no angular momentum transport

This is the most simple assumption, when no angular momentum is transported the rotation velocity should decrease with the factor $c(M)$ with which the radius increases. Hence if there would be no angular momentum transport in the star this would imply no mixing through the surface layers during the main sequence evolution.
But convection is a common phenomena in stars, and hence is mixing of the layers. Since mixing transports angular momentum it would be against common theory if the stars would have no angular momentum transport.
In Figure 4.1 it is clear that the average velocity of the calculated distribution, based on the assumption of no angular momentum transport, is much lower than the average velocity of the observed late distribution. This implies that the assumption of no angular momentum is not good for massive main sequence stars between 12 - 20 $M_{\odot}$. There has to be some kind of angular momentum transport, hence some kind of mixing process. The most likely two are convection and rotationally induced mixing.

4.2.2 Rigid rotator - instantaneous angular momentum transport

The stars would be rigid rotators if there would be instantaneous angular momentum transport throughout the star. Or at least the timescale of this transport of angular momentum should be much smaller then the time on the main sequence, which is 90% of their total lifetime, and therefore the nuclear timescale. If the angular momentum transport would be due to mixing on a basis of convection, this should not be a bad assumption, because convection occurs on much smaller timescales.
The assumption of the rigid rotator should lead to an upper limit for the velocity distribution. The core contracts during the main sequence evolution, the envelope expands. The effect is that the angular momentum in the core rotates faster and the envelope slows down, this effect could be cancelled by angular momentum transport from the core to the envelope due to mixing. If the star would be a rigid rotator, this transport would be instantaneously and the angular momentum would be balanced, until core and envelope would rotate with the same angular velocity.
In this case this balancing of angular momentum leads to a small increase of the surface velocity during the main sequence evolution.

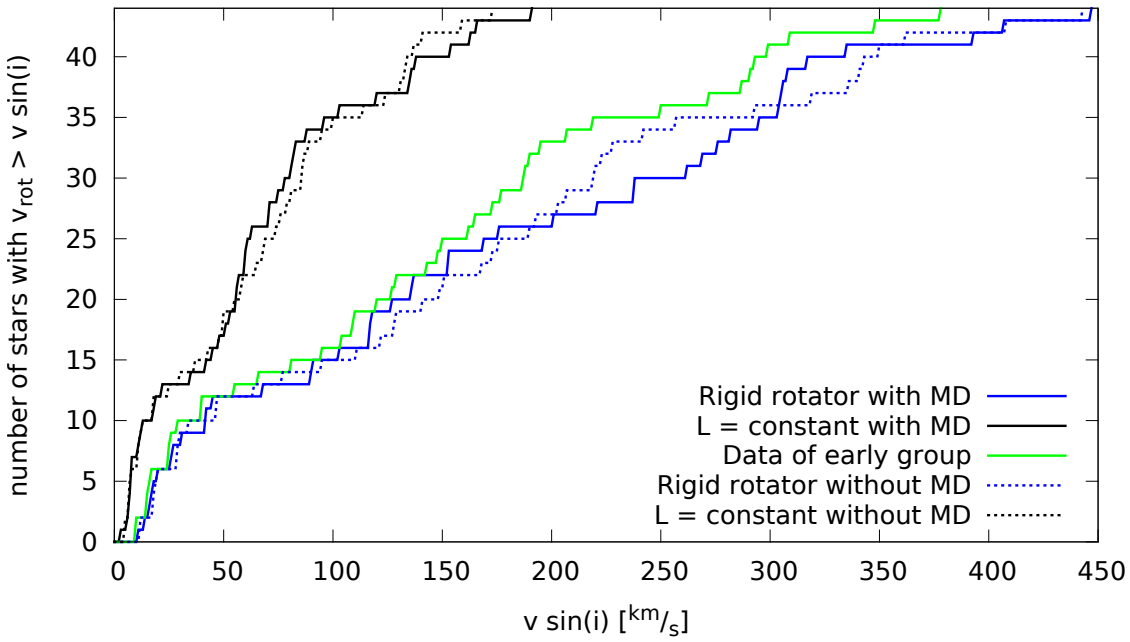

Figure 4.2: On the vertical axis is the number of stars with a bigger rotational surface velocity than then the velocity on the horizontal axis. The green solid line displays the observed rotational velocity distribution of the early group, the black solid line the distribution for the assumption of no angular momentum transport, the blue solid line shows the distribution for the assumption of a rigid rotator, both with mass dependence (MD) of the rotational velocity change factors $c(M)$ and $inte(M)$. The dotted lines represent the calculated distributions without mass dependence (MD), the blue dotted line represents a distribution for the assumption of a rigid rotator with $inte(M)$ and $c(M)$ being constant in mass, and the black dotted line shows the distribution for the assumption of no angular momentum transport with a constant $c(M)$. The solid lines are the same as shown in Figure 4.1.

4.2.3 Mass dependence

The rotational velocity change factors $c(M)$ and $inte(M)$ have a mass dependence. To treat this mass dependence in this thesis, the whole star sample had to be binned in the mass. This reduces the number of stars in each bin significantly, as seen in Table 3.2 and therefore increases the Poisson errors of the average radii, which are proportional to $\frac{1}{\sqrt{N(M)}}$ where $N(M)$ is the number of stars in the mass bin with mass M.
Therefore it is interesting if the dependence in the mass is strong enough to legitimate the division in small mass bins. Therefore the average radii has been calculated for all stars, without binning early and late group into mass bins. This results in a constant expansion factor c. The $inte(M)$ factors have been averaged and the result is a constant, not mass depended, $inte$ factor. These mass independent factor where used to calculate both distributions, seen in Figure 4.2, for both assumptions without the mass dependence.
In this sample the mass dependence seems rather small, for the assumption of no angular momentum transport, the black lines in Figure 4.2, there is almost no change in the distribution. For the assumption of a rigid rotator, blue lines in Figure 4.2, the mass dependence only occurs for fast rotator with rotational velocities bigger than 200 km s^{-1}.

4.2.4 Stellar evolution models

In addition of the two extreme assumptions the change of the rotational surface velocity has been predicted by the models of Brott et al. (2011). For each star in the early group a model of roughly the same rotational surface velocity and mass was taken, then the rotational velocity for a model number where the models radius equals the radius of the star in the early group shall be $v_{rot,E,i}$. When the model star reaches the average radius of the late group, the corresponding rotational velocity shall be $v_{rot,L,i}$. Now the rotational velocity change m_i, for this one star i, according to the models is

$$m_i = \frac{v_{rot,L,i}}{v_{rot,E,i}}. \tag{4.1}$$

Note that this change factor m_i is different for each star in the early group.

The distribution predicted by this rotational velocity change factor m_i is shown in Figure 4.1 in red. This distribution does not differ much from the observed data and predicts only a very little change in the rotational velocity during the main sequence evolution of these massive stars. A trend is may be recognized, for slow rotating stars, below 200 km s^{-1} the rotational velocity further decreases, while for those stars rotating faster than 200 km s^{-1} the rotation velocity slightly increases.
One effect to explain this behaviour could be the rotation induced mixing which is more effective in fast rotating stars, and is believed to transport angular momentum. As already seen in the discussion of the rigid rotator assumption, if the transport of angular momentum is fast and through the whole star, the rotational velocity is likely to increase during the main sequence evolution.
If the star is a slow rotator rotational induced mixing seems not effective enough to transport enough angular momentum and the star slows down during its evolution. The limit for the rotation velocity is roughly 200 km s^{-1} for the models of Brott et al. (2011).

4.3 Conclusions

Both assumptions are extreme cases. The assumption of no angular momentum transport does not fit the observed distribution. The distributions average velocity is too low to match the observations. Hence there must be any kind of angular momentum transport in the stars, and further more into the surface layer of the star, since only the surface rotation velocity can be observed.

The assumption of a rigid rotator does not fit the observations either. The distributions average velocity is not only too high, but also higher then the average observed start velocity. Therefore the angular momentum transport cannot be instantaneously, and there has to be a limit. The core has to be faster than the envelope, the stars have to rotate differential inside.

The rotational velocity of a rigid rotating star, could increase during the main sequence evolution. This holds only for the assumption that mixing of the initial angular momentum in the star is the only process that has an effect on this rotational velocity change. There are several processes occurring in massive main sequence stars that could have an effect on the rotational velocity change.
In 2.3.2 the loss of angular momentum through mass loss has been discussed. The loss of angular momentum that was transported to the surface would lead to a decreasing rotational velocity. If the star would have strong magnetic fields at the surface, magnetic breaking, discussed in 2.3.3, would lead to a decrease in the rotational surface velocity.
These processes could shift the predicted distributions to lower velocities, because these processes where not treated in this thesis they could shift the predicted distribution for the assumption of a rigid rotator to slower velocities and it could fit the observational data.

In Langer (2012b) the high probability of massive stars being in a binary system with interactions, or even merger products is discussed. Furthermore would a merger product most likely rotate much faster than a the to stars in the binary system. This star would be observed as a single star, with a high rotation velocity. This effect could shift the distributions in Figure 4.1 to higher rotational velocities.

The rotational velocity change predicted by the models of Brott et al. (2011) is not sufficient to reproduce the observed distribution of rotation velocities. Based on the models the distribution should not change much, and for fast rotators the rotational velocity should increase, while the rotational velocity should decrease for slow rotators. But according to the observed rotational velocity distribution the rotational velocity of all stars should decrease significantly for all stars with an initial rotational velocity higher than roughly 50 km s^{-1}.

It is necessary to keep the unknown margins of error in mind when interpreting these distributions. The Poisson error would decrease with the square root of the number of stars in the sample, but the errors on the observational data are unknown and of course the theoretical distributions are calculated on base of stellar evolution models that only include what we know of stars, there is room for errors too.

Acknowledgements

At last I wanted to thank everyone that helped me during my work on this thesis. And since this was my first scientific work I needed a lot of help.

Prof. Dr. Norbert Langer

He was my Supervisor and inspired me for this work.
Last year I started to visit his lecture on stars and stellar evolution and after completing it, decided to do my bachelor thesis under his supervision.
He was both friendly and help full, his door was always open and he had lots of ideas and thoughts that helped me to find the red line in this thesis, that I accidentally lost a lot of times.

Dr. Ilka Petermann

She was, so to say, my second supervisor and helped me through most of the technical problems I could not resolve myself. And She helped me a lot with the final writing too. She was the one I bothered most of the time when Norbert was busy, or out of town.

Fabian Schneider

I know him since he was my tutor in the introduction into extra galactic astronomy in my second term and he always tried to help when I had a question, problem or was confused by something. He also made it possible for me to use the data from Ines Brott by providing me with the relevant database.

Sascha Heupel

We both wrote our bachelor thesis under the supervision of Norbert at the same time, with similar topics. We studied along each other for 3 years by now and have become close friends. Since we live together he helped me a lot with the thinking processes. And since he could not run away, he was always there for me!

Lars Krause

He holds the same space in my life as Sascha, the only difference is : He got another supervisor for his bachelor thesis, but also helped me with some problems and with motivation.

Bibliography

Brott, I., de Mink, S. E., Cantiello, M., Langer, N., de Koter, A., Evans, C. J., Hunter, I., Trundle, C., and Vink, J. S. (2011). Rotating massive main-sequence stars. I. Grids of evolutionary models and isochrones. 530:A115.

de Mink, S. E. (2010). Stellar evolution at low metallicity under the influence of binary interaction and rotation .

Evans, C. J., Smartt, S. J., Lee, J.-K., Lennon, D. J., Kaufer, A., Dufton, P. L., Trundle, C., Herrero, A., Simón-Díaz, S., de Koter, A., Hamann, W.-R., Hendry, M. A., Hunter, I., Irwin, M. J., Korn, A. J., Kudritzki, R.-P., Langer, N., Mokiem, M. R., Najarro, F., Pauldrach, A. W. A., Przybilla, N., Puls, J., Ryans, R. S. I., Urbaneja, M. A., Venn, K. A., and Villamariz, M. R. (2005). The VLT-FLAMES survey of massive stars: Observations in the Galactic clusters NGC 3293, NGC 4755 and NGC 6611. 437:467–482.

Langer, N. (2012a). Nucleosynthesis. Lecture notes to the nucleosynthesis lecture in the summer term at the Universität Bonn by N. Langer.

Langer, N. (2012b). Presupernova Evolution of Massive Single and Binary Stars. 50:107–164.

Pols, E. R. (2009). Stellar Structure and Evolution. Provided in a lecture by Norbert Langer WS 2012/2013.

Appendix A

Data

All stars used for this thesis have been listed.

Table A.1: A list of tables of stars, and the group these stars are in.

Table	Group
A.1	early
A.2	late
A.3	not used
A.4	not used
A.5	not used
A.6	not used

The first two columns are used to identify the star, the most interesting parameters are displayed in the second and third column, the logarithm of the effective temperature and the logarithm of the luminosity in solar luminosity. For thesis the rotational velocities on the surface where very important, the are displayed in column five.

Table A.2: These stars are in the early group.

Cluster	Star ID	$log(T_{eff})$	$log\left(\frac{L}{L_\odot}\right)$	v_{rot} $[\frac{km}{s}]$
346	24	4.589	4.559	190
346	43	4.713	4.519	10
346	56	4.545	4.491	15
346	62	4.453	4.473	25
346	66	4.59	4.551	129
346	68	4.513	4.505	378
346	70	4.433	4.484	109
346	77	4.65	4.562	177
346	79	4.369	4.47	293
346	90	4.56	4.543	188
346	93	4.53	4.537	187
346	94	4.277	4.455	40
346	103	4.257	4.47	10
346	104	4.409	4.525	17
346	107	4.4	4.555	55
346	111	4.233	4.472	150
346	112	4.36	4.537	143
346	114	4.129	4.436	287
346	115	4.337	4.519	162
346	116	4.149	4.451	15
330	39	4.721	4.519	120
330	41	4.637	4.505	127
330	43	4.637	4.519	250
330	46	4.637	4.531	165
330	49	4.641	4.544	40
330	52	4.6	4.553	291
330	53	4.421	4.472	66
330	55	4.461	4.491	219
330	57	4.341	4.462	104
330	70	4.289	4.472	348
330	72	4.285	4.472	81
330	74	4.353	4.505	29
330	91	4.253	4.505	272
330	98	4.181	4.489	148
330	104	4.189	4.505	309
330	123	4.577	4.544	26
330	124	4.417	4.491	95
11	108	4.733	4.507	25
11	114	4.701	4.512	299
11	120	4.629	4.498	207
11	122	4.617	4.519	173
11	123	4.58	4.542	110
2004	58	4.804	4.525	195
2004	90	4.644	4.512	16

Table A.3: These stars are in the late group.

Cluster	Star ID	$log(T_{eff})$	$log\left(\frac{L}{L_\odot}\right)$	v_{rot} $[\frac{km}{s}]$
346	8	4.961	4.436	299
346	12	4.773	4.384	30
346	13	4.793	4.407	120
346	15	4.793	4.436	45
346	21	4.605	4.401	15
346	39	4.513	4.412	20
346	41	4.461	4.397	144
346	52	4.389	4.417	12
330	25	4.641	4.417	178
330	42	4.381	4.406	26
11	34	5.029	4.407	203
11	36	4.945	4.376	55
11	54	4.785	4.371	60
11	56	4.893	4.428	205
11	69	4.633	4.386	80
11	76	4.669	4.423	97
11	78	4.589	4.39	93
11	82	4.58	4.41	95
11	88	4.538	4.383	240
11	90	4.532	4.389	104
11	94	4.502	4.383	147
11	96	4.494	4.383	32
11	98	4.373	4.336	45
11	103	4.528	4.41	125
11	104	4.524	4.41	153
11	107	4.508	4.41	80
11	109	4.481	4.411	55
11	110	4.373	4.364	25
11	111	4.356	4.361	101
11	115	4.39	4.383	53
2004	23	4.852	4.39	102
2004	24	4.723	4.361	240
2004	25	4.748	4.39	83
2004	26	4.677	4.36	19
2004	29	4.649	4.364	30
2004	35	4.737	4.428	244
2004	39	4.671	4.41	212
2004	43	4.519	4.361	24
2004	44	4.619	4.41	18
2004	46	4.617	4.416	32
2004	48	4.49	4.369	173
2004	56	4.523	4.41	229
2004	66	4.475	4.41	238
2004	67	4.475	4.41	237
2004	71	4.331	4.361	98
2004	89	4.306	4.369	288
2004	92	4.344	4.39	171

Table A.4: These stars where not used in this thesis.

Cluster	Star ID	$log(T_{eff})$	$log\left(\frac{L}{L_\odot}\right)$	v_{rot} $[\frac{km}{s}]$
346	1	6.02	4.533	74
346	4	5.165	4.436	266
346	7	5.45	4.631	120
346	9	5.077	4.505	199
346	10	5.2	4.555	313
346	16	4.869	4.472	181
346	18	5.1	4.515	138
346	20	4.685	4.436	34
346	22	4.95	4.566	55
346	23	4.805	4.489	65
346	25	4.9	4.559	138
346	26	4.845	4.512	75
346	27	4.781	4.491	220
346	28	5.1	4.632	27
346	29	4.817	4.507	25
346	30	4.813	4.505	183
346	31	4.99	4.597	18
346	32	4.677	4.462	125
346	33	4.99	4.601	188
346	35	4.605	4.436	145
346	36	4.685	4.472	287
346	37	4.205	4.274	35
346	40	4.673	4.486	20
346	44	4.325	4.362	40
346	45	4.557	4.472	181
346	46	4.81	4.599	340
346	47	4.153	4.298	63
346	48	4.153	4.301	158
346	49	3.697	4.114	80
346	50	4.67	4.571	357
346	51	4.87	4.619	18
346	53	4.513	4.47	170
346	54	4.405	4.436	23
346	55	4.485	4.47	130
346	57	4.085	4.298	73
346	58	4.469	4.47	180
346	61	4.317	4.417	336
346	64	4.309	4.417	108
346	65	4.049	4.301	222
346	67	4.293	4.417	351
346	69	4.277	4.417	186
346	72	4.261	4.417	102
346	73	4.261	4.417	190
346	74	3.801	4.217	52
346	75	4.313	4.442	10
346	76	4.209	4.397	237
346	78	4.045	4.326	154
346	80	4.289	4.439	216
346	81	4.033	4.326	255
346	82	4.033	4.326	168
346	83	4.277	4.436	207
346	84	4.273	4.436	105
346	85	4.025	4.326	26
346	88	4.261	4.436	84
346	89	4.213	4.417	79
346	91	4.249	4.436	49
346	92	4.241	4.436	234
346	95	4.181	4.417	227
346	96	4.181	4.417	343
346	97	4.75	4.574	22
346	98	4.161	4.417	68
346	99	3.789	4.255	80
346	100	4.157	4.417	183
346	101	4.181	4.436	29
346	102	3.749	4.248	112
346	106	4.169	4.439	142
346	108	4.113	4.417	167
346	109	4.113	4.417	123
346	110	4.109	4.417	243
330	2	4.761	4.164	14
330	3	4.885	4.236	49
330	4	4.809	4.23	36
330	5	4.577	4.137	16
330	9	4.445	4.144	29
330	10	4.441	4.171	0
330	13	5.4	4.538	73
330	14	4.685	4.304	81

Table A.5: These stars where not used in this thesis.

Cluster	Star ID	$log(T_{eff})$	$log\left(\frac{L}{L_\odot}\right)$	v_{rot} $[\frac{km}{s}]$
330	16	4.241	4.152	40
330	17	4.661	4.342	14
330	18	4.449	4.255	46
330	20	4.349	4.223	44
330	21	4.949	4.484	204
330	22	4.421	4.276	23
330	24	4.053	4.146	45
330	26	4.497	4.352	71
330	27	4.461	4.343	80
330	28	4.633	4.436	76
330	29	4.753	4.489	209
330	31	4.693	4.471	178
330	32	4.669	4.473	17
330	33	4.533	4.417	105
330	34	4.529	4.417	231
330	35	4.217	4.279	37
330	36	4.325	4.326	37
330	38	4.525	4.436	150
330	40	4.249	4.326	106
330	44	4.365	4.417	184
330	45	4.009	4.266	133
330	47	4.345	4.427	28
330	48	4.421	4.462	73
330	50	4.045	4.301	214
330	51	4.301	4.417	273
330	54	4.245	4.397	147
330	56	4.061	4.326	108
330	58	3.913	4.301	263
330	59	3.885	4.266	123
330	60	4.081	4.352	88
330	62	3.949	4.301	241
330	63	4.117	4.397	199
330	64	3.925	4.301	269
330	65	4.129	4.397	284
330	66	3.833	4.267	126
330	67	3.901	4.298	65
330	68	4.157	4.417	23
330	69	3.845	4.279	193
330	71	3.841	4.279	92
330	73	3.373	4.079	51
330	75	3.461	4.13	122
330	76	3.861	4.301	62
330	79	3.817	4.29	146
330	80	4.057	4.397	283
330	81	3.785	4.279	190
330	82	4.053	4.397	192
330	83	3.721	4.255	140
330	84	3.829	4.301	26
330	85	3.821	4.301	191
330	86	3.801	4.298	89
330	87	3.805	4.301	214
330	89	3.701	4.267	193
330	90	3.689	4.266	167
330	94	3.765	4.301	330
330	95	3.673	4.266	20
330	96	3.973	4.397	175
330	97	4.049	4.436	154
330	99	3.861	4.352	187
330	100	3.993	4.417	373
330	101	3.725	4.298	48
330	102	3.717	4.298	129
330	103	3.937	4.397	131
330	105	3.913	4.397	13
330	106	3.949	4.417	71
330	107	3.485	4.217	34
330	108	3.349	4.161	102
330	109	3.601	4.266	213
330	110	3.737	4.326	110
330	111	3.793	4.352	173
330	112	3.789	4.352	262
330	113	3.781	4.352	327
330	114	3.833	4.377	17
330	116	3.617	4.29	4
330	118	3.889	4.417	32
330	119	3.841	4.397	265
330	120	3.473	4.267	137

Table A.6: These stars where not used in this thesis.

Cluster	Star ID	$log(T_{eff})$	$log\left(\frac{L}{L_\odot}\right)$	v_{rot} $[\frac{km}{s}]$
330	125	4.009	4.326	86
11	1	5.657	4.273	50
11	2	5.261	4.199	55
11	3	5.421	4.365	80
11	4	5.8	4.5	81
11	8	5.393	4.406	75
11	9	4.845	4.176	40
11	10	5.589	4.505	152
11	11	5.489	4.47	86
11	12	5.129	4.312	70
11	14	5.025	4.281	50
11	15	5.229	4.373	75
11	16	5.125	4.336	60
11	17	4.821	4.217	45
11	23	5.085	4.38	70
11	24	4.961	4.334	55
11	26	5.92	4.727	109
11	29	5.21	4.459	70
11	31	5.84	4.653	116
11	32	5.43	4.547	96
11	33	5.07	4.435	256
11	35	5.229	4.491	94
11	37	5.081	4.449	100
11	38	5.69	4.613	145
11	39	4.813	4.336	157
11	40	5.113	4.47	273
11	42	5.053	4.462	30
11	45	5.15	4.509	105
11	46	5.205	4.525	205
11	47	5.029	4.465	55
11	48	5.38	4.61	130
11	51	5.31	4.627	333
11	52	5.225	4.544	16
11	58	5.27	4.616	85
11	59	5.125	4.531	103
11	60	5.57	4.66	106
11	61	5.2	4.526	87
11	62	4.953	4.483	25
11	63	5.109	4.544	196
11	64	4.917	4.481	206
11	65	5.17	4.62	83
11	66	5.1	4.594	71
11	68	5.06	4.601	54
11	70	4.401	4.29	79
11	72	4.773	4.459	15
11	73	4.777	4.464	222
11	74	4.777	4.464	169
11	75	4.481	4.338	25
11	77	4.465	4.332	117
11	79	4.877	4.512	38
11	81	4.793	4.497	363
11	83	4.705	4.467	20
11	84	4.745	4.47	108
11	85	4.729	4.464	105
11	86	4.647	4.428	75
11	87	4.91	4.515	276
11	89	4.421	4.336	117
11	93	4.289	4.29	73
11	95	4.591	4.428	267
11	97	4.165	4.243	51
11	100	4.677	4.473	30
11	101	4.675	4.474	70
11	102	4.725	4.491	218
11	105	4.559	4.428	116
11	106	4.717	4.494	25
11	113	4.49	4.426	38
11	116	4.281	4.336	160
11	117	4.463	4.428	247
11	118	4.42	4.41	150
11	119	4.42	4.41	259
11	121	4.451	4.428	265
11	124	4.469	4.455	45
2004	3	5.042	4.16	42
2004	5	4.954	4.093	31
2004	7	4.899	4.088	25
2004	10	5.016	4.235	45

Table A.7: These stars where not used in this thesis.

Cluster	Star ID	$log(T_{eff})$	$log\left(\frac{L}{L_\odot}\right)$	v_{rot} $[\frac{km}{s}]$
2004	11	5.219	4.327	62
2004	12	4.92	4.328	47
2004	13	4.936	4.336	165
2004	14	4.722	4.25	20
2004	15	4.959	4.361	170
2004	20	4.907	4.361	149
2004	21	4.818	4.331	59
2004	22	4.792	4.338	42
2004	27	4.999	4.497	182
2004	30	4.865	4.462	123
2004	31	4.58	4.336	66
2004	32	4.576	4.336	111
2004	36	4.576	4.336	42
2004	41	4.428	4.311	101
2004	42	4.45	4.322	42
2004	45	4.456	4.336	128
2004	47	4.416	4.336	133
2004	50	4.352	4.311	109
2004	51	4.404	4.336	70
2004	52	4.396	4.336	138
2004	53	4.775	4.498	7
2004	54	4.392	4.336	114
2004	55	4.332	4.311	118
2004	59	4.352	4.336	91
2004	60	4.352	4.336	134
2004	61	4.31	4.322	40
2004	62	4.667	4.481	106
2004	63	4.324	4.336	107
2004	64	4.482	4.413	28
2004	65	4.252	4.311	223
2004	68	4.248	4.311	62
2004	69	4.541	4.447	178
2004	70	4.514	4.438	46
2004	73	4.264	4.336	37
2004	74	4.485	4.437	130
2004	75	4.264	4.336	116
2004	76	4.204	4.311	37
2004	77	4.561	4.47	215
2004	78	4.26	4.336	115
2004	79	4.26	4.336	165
2004	80	4.192	4.311	85
2004	81	4.453	4.428	105
2004	82	4.415	4.41	161
2004	83	4.415	4.41	194
2004	84	4.461	4.438	36
2004	85	4.18	4.311	150
2004	86	4.236	4.336	14
2004	87	4.399	4.41	35
2004	88	4.176	4.311	200
2004	91	4.42	4.424	40
2004	93	4.138	4.301	189
2004	94	4.156	4.311	84
2004	95	4.379	4.41	138
2004	96	4.375	4.41	245
2004	97	4.2	4.336	62
2004	98	4.2	4.336	90
2004	99	4.192	4.336	119
2004	100	4.381	4.428	323
2004	101	4.176	4.336	131
2004	102	4.176	4.336	64
2004	103	4.176	4.336	35
2004	104	4.335	4.41	274
2004	105	4.335	4.41	235
2004	106	4.172	4.336	41
2004	107	4.428	4.455	146
2004	108	4.208	4.354	13
2004	109	4.108	4.311	41
2004	110	4.168	4.336	121
2004	111	4.08	4.311	55
2004	112	4.14	4.336	72
2004	113	4.08	4.311	307
2004	114	4.124	4.336	59
2004	115	4.24	4.39	8
2004	116	4.12	4.336	63
2004	117	4.108	4.336	75
2004	118	4.251	4.41	90
2004	119	4.15	4.366	15

Ich versichere, dass ich diese Arbeit selbständig verfasst und keine anderen als die angegebenen Quellen und Hilfsmittel benutzt sowie die Zitate kenntlich gemacht habe.

Bonn, den…….. Unterschrift……

Auf dem Deckblatt der Arbeit müssen die folgenden formalen Inhalte stehen: Titel/Thema, Bachelorarbeit in Physik von (Ihr vollständiger Name), angefertigt im Institut (Name des Instituts), vorgelegt der Mathematisch-Naturwissenschaftlichen Fakultät der Universität Bonn, Monat und Jahr der Abgabe (z. B. August 2012).

Auf einer der ersten Innenseiten schreiben Sie bitte noch, wer Ihre Gutachter sind:
1. Gutachter(in): vollständiger Name (das wird der Betreuer, die Betreuerin sein),
2. Gutachter(in): vollständiger Name (Ihr Vorschlag, abgesprochen mit Ihrem Betreuer, Ihrer Betreuerin).
Achtung: Eine/einer von beiden muss gemäß § 18, Abs. 2 BPO Mitglied der Gruppe der Hochschullehrer und Hochschullehrerinnen sein, also Professor/Professorin oder Privatdozent/Privatdozentin.

Stand: 7. Oktober 2011